Prediction of the ultimate strength of quasi-isotropic TP-based laminates structures from tensile and compressive fracture toughness at high temperature

Benoît Vieille, Juan Daniel Pujols Gonzalez, Christophe Bouvet

Prediction of the ultimate strength of quasi-isotropic TP-based laminates structures from tensile and compressive fracture toughness at high temperature

B. Vieille[a,*], J.-D. Pujols Gonzalez[a], C. Bouvet[b]

[a] INSA Rouen, Groupe de Physique des Matériaux (UMR CNRS 6634), 76801, St Etienne du Rouvray, France
[b] Institut Clément Ader (UMR CNRS 5312), Université de Toulouse, ISAE-SUPAERO, 10 av. E. Belin, 31055, Toulouse cedex 4, France

Keywords:
Thermoplastic
Fracture mechanics
Failure
Microbuckling
High-temperature

A B S T R A C T

This paper is intended to test the capacity of a simple model based on fracture mechanics concepts to predict the ultimate strength of notched hybrid carbon and glass fibers woven-ply reinforced PolyEther Ether Ketone (PEEK) thermoplastic (TP) quasi-isotropic (QI) laminates under different temperature conditions. In such materials, translaminar failure is the primary failure mode driven by the breakage of 0° and 45° oriented fibers in tension as well as the formation of kink-band in compression. Single-Edge-Notched Bending (SENB), Open-Hole-Tensile (OHT) and Open-Hole-Compression (OHC) specimens have been conducted at room temperature (RT) and at a temperature higher than the glass transition temperature (T_g). The Critical Damage Growth model derived from the Average Stress Criterion and Linear Elastic Fracture Mechanics (LEFM) have been applied to open-hole specimens to determine the critical damage zone from which the fracture toughness in tension (0° and 45° fibers breakage) $K_{Ic}^{tension}$ and in compression (kink-band formation) $K_{Ic}^{comp.}$ are estimated. In Single Edge Notched Bending (SENB) specimens experience simultaneous tension/compression. From the estimation of $K_{Ic}^{tension}$ and $K_{Ic}^{comp.}$, the ultimate strength of SENB specimens can be predicted. LEFM equations combined with the critical fracture toughness in tension give relatively accurate results, suggesting that failure is driven by fibers bundles breakage in tension.

1. Introduction

The design of composites structures with high gradient of stresses has been extensively studied over the past fifty years. So far, there is no clear cut answer regarding the failure criteria of laminated composites as they may experience many failure modes (matrix cracking, fiber/matrix debonding, fiber breakage, delamination) which may interact and complicate the study of damage growth within the laminates' layers but also between the layers. Thus, many analytical techniques ranging from complex numerical methods to simplified semi empirical fracture models have been proposed in the literature to predict the ultimate strength of composite structures [1]. Among the semi empirical approaches simple to implement [2 11], most of them deal with tension or compression loadings. The most commonly used criteria are Point Stress Criterion (PSC) and Average Stress Criterion (ASC) initially developed by Whitney and Nuismer [10,11]. These criteria have been successfully applied to composites by many authors [1,9,12,13]. Similarly, Waddoups et al. assumed the existence of damaged (inherent flaw) regions whose size c is modelled as a through crack of constant length developing at the edges of the hole in the transverse direction [4,14]. Bowie et al. applied this model to isotropic and homogeneous materials [15]. Based on an effective crack growth model [16], Bel monte developed a Critical Damage Growth model for evaluating the residual strength of open hole composite laminates [5]. This model is physically meaningful, as it only requires the knowledge of the strength of the unnotched laminates and an estimate of the mode I critical fracture toughness of the laminate. Early in the sixties Wu showed that the concepts of fracture mechanics developed for isotropic materials can be applied to unidirectional composite materials provided a few conditions are fulfilled such as the orientation of the notch with respect to the orthotropic axis. In addition, the stress intensity factors of orthotropic materials must be consistent with the isotropic case in stress distribution and in crack displacement modes [17]. According to Waddoups et al., the damage state of the material in the region of intense macroscopic stresses is unknown due to material heterogeneity [14]. However, the material's fracture toughness is assumed constant

* Corresponding author.
E-mail address: benoit.vieille@insa-rouen.fr (B. Vieille).

https://doi.org/10.1016/j.compositesb.2019.01.056

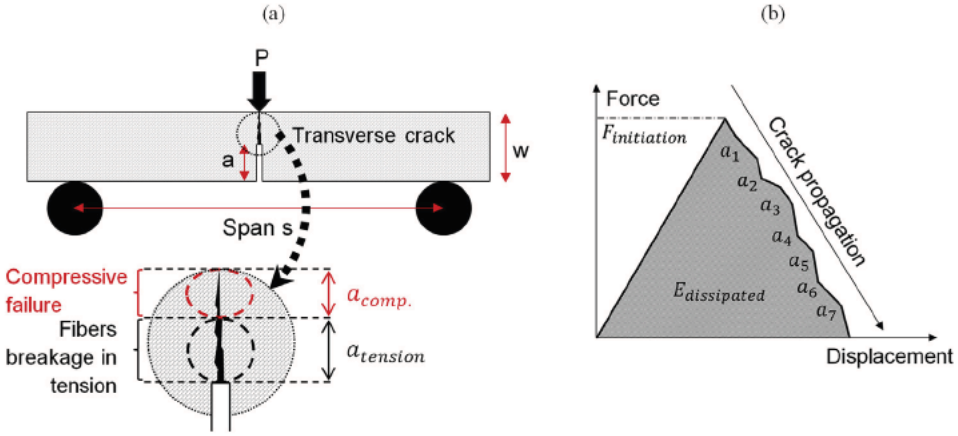

Fig. 1. Failure in bending: (a) simultaneous failure in compression and tension – (b) Dissipated fracture energy along with crack propagation.

for a transverse crack and may be obtained from the strain energy release rate G which is expected to be a function of laminate stacking sequence. To the author's best knowledge, simplified semi empirical fracture models have been only applied to open hole tensile specimens but never to single edge notch specimens.

One of the main drawbacks of the previous models is their incapability to account for size effects [18]. Camanho et al. compared a continuum damage model with alternative approaches: the point stress criterion, the inherent flaw model, the Linear Elastic Fracture Mechanics and the strength of materials approaches. Their results show that a continuum damage model is the most accurate technique to predict the ultimate strength and the size effects of notched composites. In addition, it does not require any calibration and it is applicable to general geometries and boundary conditions. However, it is based on finite element computations and it is not straightforward to apply from experimental results.

1.1. Experimental evaluation of the mode I critical fracture toughness

Most of the simplified semi empirical fracture models require the estimate of the mode I critical stress intensity factor K_{Ic} which is usually derived from analytical functions depending on specimens geometries and loading conditions [19]:

$$K_{Ic} = \sigma_{remote}\sqrt{\pi a}\,.\,F(a/w) \tag{1}$$

where σ_{remote} is the remote applied stress, a denotes the length of the initial crack and w is the specimen width [4]. $F(a/w)$ is a geometric finite width correction (FWC) function [20]. In Single Edge Notch Bending (SENB) specimens, $F(a/w)$ is obtained from an empirical formula classically used in the literature [20]:

$$F(a/w) = \frac{1}{\sqrt{\pi}}.\frac{[1.99 - (a/w)(1 - a/w)(2.15 - 3.93.\,a/w + 2.7.\,(a/w)^2]}{(1 + 2.\,a/w)(1 - a/w)^{3/2}} \tag{2}$$

Finally, the stress concentration factor K_t for Mode I type loading [4,20] is defined by:

$$K_t = \frac{\sigma_y(r, \theta = 0)}{\sigma_{remote}} = \sqrt{\frac{a}{2r}}\,.\,F(a/w) \tag{3}$$

where r is the radius of the notch at the crack tip and σ_{remote} is the remote applied stress far from the notch.

From the knowledge of the critical fracture toughness in tension or compression, the ultimate strength of SENB specimens can be predicted from Eq. (2):

$$\sigma^u_{remote} = \frac{K_{Ic}^{tension\ or\ compression}}{\sqrt{\pi a}\,.\,F(a/w)} \tag{4}$$

At initiation, LEFM equations can be applied to quantify tensile failure (associated with the breakage of 0° fibers) as the thermo mechanical response is elastic quasi brittle to estimate $K_{Ic}^{tension}$. However, it is a strong approximation to apply them in the case of compressive failure as the formation of kink bands and the crushing of 0° fibers are the primary failure mechanisms for which the mechanical behavior is not linear anymore [21]. Thus, LEFM was applied to account for the unstable kink band growth when the stress intensity factor at the kink band tip is higher than the critical compressive fracture toughness $K_{Ic}^{comp.}$ associated with the kink band formation.

Compact tension and compact compression specimens are classically used to estimate the fracture toughness associated with the translaminar failure of 0° fibers in tension (fibers breakage) $K_{Ic}^{tension}$ and in compression (kink band formation) $K_{Ic}^{comp.}$ [22 26]. However, the obtained values are very sensitive to specimen's geometry and these tests require specific tools to be clamped to the grips of the testing machine. These specimens are also prone to twisting and buckling when subjected to tension and compression respectively. Thus, it is more straightforward to conduct tensile and compressive tests on open hole specimens with different hole diameters to estimate $K_{Ic}^{tension}$ and $K_{Ic}^{comp.}$.

In orthotropic materials, the strain energy release rate G_I and the stress intensity factor K_I are related to the engineering constants as follows [27]:

$$G_{Ic} = C_I.\,(K_{Ic})^2 \tag{5}$$

with $C_I = \sqrt{\frac{1}{2E_xE_y}}\sqrt{\sqrt{\frac{E_x}{E_y}} - \nu_{xy} + \frac{E_x}{2G_{xy}}}$ in plane stress conditions. As is based on the assumption of a linear elastic behavior, this relationship is rather well fulfilled in the case of a tensile failure. As was previously underlined, the use of Eq. (5) is a strong approximation in the case of a compressive failure.

Failure primarily consists of simultaneous tensile breakage of 0° fibers and compressive kinking of 0° fibers in SENB specimens (see Fig. 1a). $a_{tension}$ and $a_{comp.}$ are the equivalent crack lengths associated with tension and compression respectively. $E_{dissipated}$ represents the energy dissipated during fracture (see Fig. 1b).

1.2. Fracture toughness in open hole tensile specimens

The methods to estimate fracture toughness in open hole specimens differ from the one presented in the above section. For example, the simplified semi empirical fracture models introduced in section 1.1 are based upon the stable growth and subsequent catastrophic failure of a damage zone at the edge of central open hole specimens [5]. In the present case, the Critical Damage Growth (CDG) model is interesting for many reasons:

(i) the failure criterion is based on LEFM principles,

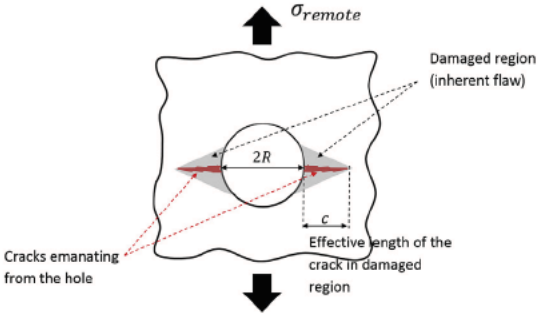

Fig. 2. Cracks emanating from the hole in laminates experiencing translaminar failure mode (Adapted from Ref. [14]).

(ii) its parameters are physically meaningful,
(iii) it can be applied to both tensile and compressive loadings.

This approach combines the remote applied stress σ_{remote}, and the corresponding critical damage zone size c which can be obtained from the Average Stress Criterion [20]. This model can be applied to quasi isotropic laminates to determine the length of the critical damage zone and to compute the mode I critical fracture toughness either in tension $K_{Ic}^{tension}$ or in compression $K_{Ic}^{comp.}$.

Firstly, the average stress criterion (ASC) assumes that failure occurs when the average stress, over a distance c, away from the notch is equal or greater than the strength of the unnotched laminate $\sigma_{unnotched}$. The effective crack length c depends on the diameter of the hole. The remote applied stress σ_{remote}; required to grow a damage zone or crack to a length c (see Fig. 2); from the edge of the hole (whose radius is r) is defined using an average stress argument and is given by:

$$\sigma_{remote} = \frac{1}{c}\int_{r}^{r+c} \sigma_y dx = \frac{1}{c}\int_{r}^{r+c} \sigma_y^{\infty}.\, F_0 dx \tag{6}$$

Where σ_y is the longitudinal strength adjacent to the notch edge in a finite plate [4] which can be determined from the analytical expression of the longitudinal strength adjacent to the notch edge in an infinite plate σ_y^{∞} [20], and a Finite Width Correction (FWC) factor $F_0 = {K_T}/{K_T^{\infty}}$. Indeed, the stress concentration factor at the edge of the hole K_T^{∞} in orthotropic infinite plates is defined from the mechanical properties of the equivalent orthotropic material (see Table 3) as follows [1,19,20]:

$$K_T^{\infty} = 1 + \sqrt{2\left[\sqrt{\frac{E_y}{E_x}} - \nu_{xy}\right] + \frac{E_y}{G_{xy}}} \tag{7}$$

In the case of orthotropic specimens with a finite width w containing a central circular hole with a diameter d, Tan has proposed the following approximate expressions of the FWC factor [20]:

$$\frac{1}{F_0} = \frac{3(1-d/w)}{2+(1-d/w)^3} + \frac{(K_T^{\infty}-3)}{2}\left[1-\left(\frac{d}{w}M\right)^2\right]\left(\frac{d}{w}M\right)^6 \tag{8}$$

where the coefficient M is obtained from the following equation:

$$M^2 = \frac{\sqrt{1-8\left[\frac{3(1-d/w)}{2+(1-d/w)^3}-1\right]}-1}{2(d/w)^2} \tag{9}$$

Secondly, the ultimate remote stress σ_{remote}^{u} required to observe a catastrophic failure in the case of cracks emanating from a circular hole (whose radius is r) is associated with the mode I critical fracture toughness K_{Ic} by the following equation [4,20]:

$$K_{Ic} = \sigma_{remote}^{u}\sqrt{\pi r}.\, F_1.\, F_2.\frac{c}{c+r} \tag{10}$$

where F_1 is a correction factor determined in the case of isotropic materials for cracks [15], whose length c is growing from a circular hole [4]:

$$F_1 = \frac{(3-s)}{2}[1+1.243*(1-s)^3] \text{with } s = \frac{c}{c+r} \tag{11}$$

and the FWC factor F_2 is given by:

$$F_2 = \sqrt{sec\left(\frac{\pi R}{2w}\right)sec\left(\frac{\pi(R+c)}{2w}\right)} \tag{12}$$

The estimation of the critical fracture toughness K_{Ic} by Eq. (10) depends on the geometry, the loading conditions and the length of the critical damage zone c [9,12].

1.3. Fracture toughness in open hole compressive specimens

In the case of Open Hole Compression tests, following an idea similar to the one proposed by Belmonte [5], Soutis developed a kink band propagation model to compute the OHC strength from the hole diameter, the unnotched compressive strength $\sigma_{unnotched}^{comp.}$ and the kink band compressive toughness [3,23 26]. The kink band growth depends on two competing mechanisms:

(i) a stable growth driven by the stress concentration near the hole and $\sigma_{unnotched}^{comp.}$
(ii) an unstable growth driven by the mode I stress intensity factor $K_I^{comp.}$ at the kink band tip and the compressive fracture toughness $K_{Ic}^{comp.}$ (see Fig. 3).

For stable kink band growth, the ASC criterion (Eq. (7)) is considered to compute the length of the critical damage zone c near the hole. In the present case, the average stress criterion stipulates that the stable kink band growth occurs when the magnitude of the average stress over the kink band (whose length is c) equals that of the unnotched laminate compressive strength $\sigma_{unnotched}^{comp.}$ [28]. The LEFM approach can be applied to account for the unstable kink band growth when the stress intensity factor at the kink band tip is higher than the compressive fracture toughness $K_{Ic}^{comp.}$ associated with the kink band formation. It is also possible to estimate $K_{Ic}^{comp.}$ by means of the micromechanics model for fiber microbuckling initially proposed by Budiansky [28,29]. Soutis considered the response of an open hole specimen subjected to a compressive loading [25,29]. The unnotched compressive strength σ_{un} of long fiber reinforced polymer composites is primarily driven by fiber microbuckling. Such microbuckling results from the plastic deformation of the polymer matrix in shear preferentially initiated in the region of fibers waviness. According to Rice [30], the energy required to extend a crack can be estimated from the stress vs crack displacement curve (see Fig. 4a) assuming that the compressive stress changes linearly with the displacement (which is a rough approximation of what is observed experimentally during compressive failure):

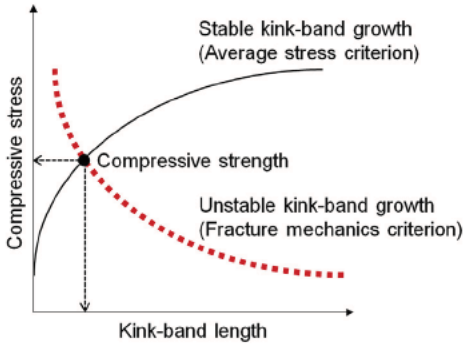

Fig. 3. Illustration of the kink-band growth competing mechanisms (Adapted from Ref. [28]).

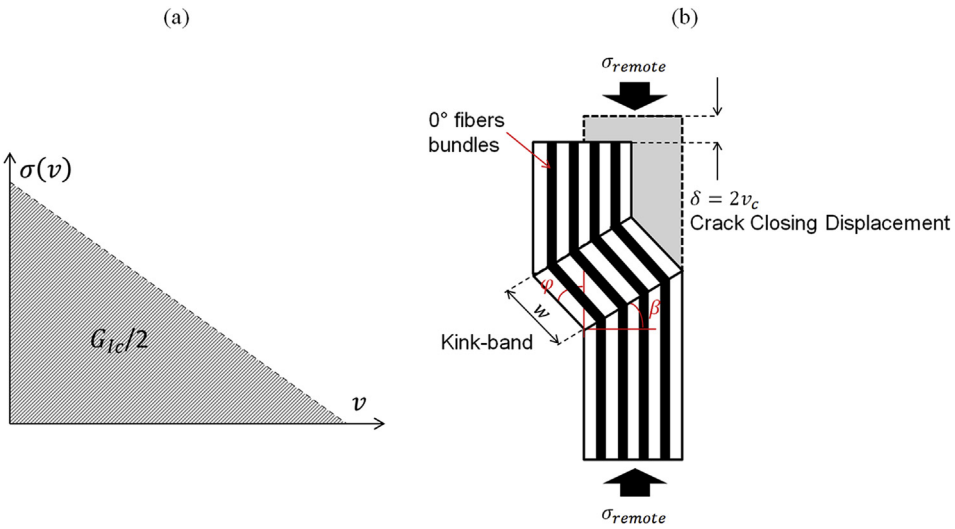

Fig. 4. (a) Evaluation of G_{Ic} from the evolution of the tensile stress along with crack closing displacement (b) Kinematics of fiber microbuckling in fiber-reinforced polymer composites.

$$G_{Ic} = 2\int_0^{v_c} \sigma(v)dv = \sigma_{un}.\, v_c \tag{13}$$

Where v_c represents the critical Crack Closing Displacement (CCD) also known as the crack overlap displacement δ_c which is associated with the formation of the kink band during the fiber rotation (see Fig. 4b). Assuming that fibers rotation φ complies with the rotation of a rigid perfectly plastic body under a compressive remote stress σ_{remote}, the critical crack overlap displacement δ_c is equal to the kink band width.

1.4. Objectives of the study

Based on LEFM equations, this study deals with the ultimate strength of Single Edge Notched Bending specimens consisting of carbon/glass/PEEK thermoplastic hybrid laminated composites. In quasi isotropic laminates, failure is expected to be driven by the breakage of 0° and 45° oriented fibers bundles in tension as well as the formation of kink band in compression. The influence of temperature on matrix ductility and fracture toughness is examined. In order to predict the ultimate strength of SENB specimens experiencing both tensile and compressive failure, it is necessary to evaluate the mode I critical fracture toughness in tension $K_{Ic}^{tension}$ and in compression $K_{Ic}^{comp.}$ whose values can be computed from the combined application of the Average Stress Criterion and LEFM equations.

2. Materials, specimens and tests procedure

2.1. Materials

The laminated plates obtained by thermo compression are made up of carbon (Tenax® E HTA40 3K) PEEK 5HS woven plies prepregs and glass PEEK prepregs (see Table 1). The consolidated laminates consist of 14 inner carbon PEEK plies and two outer glass PEEK plies [31,32]. In addition, the carbon and glass fiber fabrics are balanced in the warp and weft directions. The stacking sequence of laminates is quasi iso tropic: $[(0/90)_G,[(0/90),(\pm 45)]_3,(0/90)]s$ (with G index for glass fi bers ply). The average thickness of laminates is about 4.5 mm.

2.2. Specimens

The test specimens were cut by water jet from 600 × 600 mm^2 plates. The machining of the single edge notches in SENB specimens

Table 1
A few properties of woven carbon and glass fibers reinforced PEEK elementary ply at RT.

	Carbon/PEEK	*Glass/PEEK*
E_x (GPa)	60	22
E_y (GPa)	60	20
G_{xy} (GPa)	4.8	6.55
	0.04	0.04
Tensile strength (warp) (MPa)	963	1172
Compressive strength (warp) (MPa)	725	1103
Nominal ply thickness (mm)	0.31	0.25
Tg (°C)	143	143

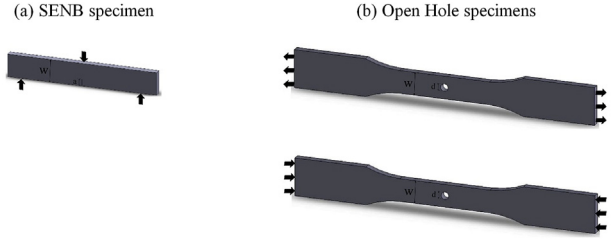

Fig. 5. Geometries of test specimens.

(see Fig. 5a) was done by means of a precision endless diamond wire saw whose radius is 0.085 mm. The initial notch length to specimen width ratio a/w ranges from 0.2 to 0.5. In OHT and OHC specimens (see Fig. 5b), central circular holes were drilled by means of a diamond tool (drill bit), which is known to minimise damage near the hole [33]. Specimens have different ratio d/w (ranging from 0.1 to 0.4) of the hole diameter over the specimen width.

2.3. Methods and experimental set up

2.3.1. Thermo mechanical testing

Open hole tensile, compressive and bending tests were performed using a 100 kN capacity load cell of a MTS 810 servo hydraulic testing machine in displacement controlled mode and with a temperature control system. Mechanical tests were applied to notched specimens at Room Temperature (RT) and 150 °C. The studied composite material being considered for applications in aeronautics (e.g. engine's nacelle), it can be used up to 150 °C > T_g of C/PEEK (=143 °C), as detailed in

Ref. [34]. The tensile mechanical properties were determined according to the European standards EN 6035 [35]. The mechanical properties of C/PEEK and G/PEEK elementary plies are specified in Table 1 [31].

2.3.2. Full field measurements

A two dimensional Digital Image Correlation (DIC) technique was used to measure full field displacements in notched laminates [36]. During thermomechanical loading, a high speed monochromic camera Phantom Miro M310 records digital images at full resolution (1280 × 800 pixels), and at a rate of 3200 frames per second. The Green Lagrange strain fields were obtained by means of the VIC 2D correlation software (provided by the company Correlated Solutions). In the present work, full field measurements will be applied to SENB specimens (with a ratio $a/w = 0.3$) to evaluate the equivalent crack lengths associated with tension and compression $a_{tension}$ and $a_{comp.}$ re spectively (cf. section 1.2).

3. Results and discussion

3.1. Tensile and compressive macroscopic thermo mechanical responses

For both testing conditions, unnotched laminates are characterized by an elastic behavior until failure in tension [32], and a slightly elastic plastic behavior in compression. Based on the standards introduced in section 2.1, the mechanical properties in tension and compression of unnotched CG/PEEK quasi isotropic laminates can be determined de pending on testing temperature (see Table 2). It appears that tem perature has moderate influence (about −10%) on longitudinal stiff ness, ultimate strength $\sigma^u_{unnotched}$ and strain at failure in tension. In compression, the influence of temperature is particularly significant on the ultimate compressive strength and the strain at failure (about −25%). From the macroscopic response standpoint, OHT specimens also exhibit elastic brittle behavior at both test temperatures [32]. Temperature influences both macroscopic mechanical response and properties of open hole specimens due to local softening of the PEEK matrix at high temperature. As ratio d/w increases, the residual strength decreases by 30 50% suggesting that the stress concentration due to the hole significantly influences its strength. Indeed, the hole sensitivity (indicated in % on Fig. 6) represents the decrease in the ultimate strength of OHT specimens with respect to the notch insensitive case (computed from the net section and the ultimate strength of the un notched specimens). It appears to be virtually the same at both tem peratures. It therefore suggests that the effect of stress concentration is temperature independent in CG/PEEK quasi isotropic laminates whose mechanical tensile response is fiber dominated.

Under compressive loading, as was observed in unnotched speci mens, the behavior of OHC specimens is elastic with noticeable plastic deformation due to the formation of local plastic kink band as further detailed in the next section (see Fig. 7). A ratio $d/w = 0.4$ was specifi cally chosen to promote the breakage of 0° fibers bundles and to avoid a macroscopic buckling. For both temperatures, the residual strength in Open Hole specimens is 65% lower than the one observed in unnotched specimens subjected to compression. The influence of the stress con centration being the same on the residual compressive strength, it tends to prove that the hole sensitivity is not temperature dependent though the local ductility of the PEEK matrix is significantly enhanced at temperature higher than its T_g. However, the effect of a temperature increase is significant on both macroscopic mechanical response and properties of OHC specimens as a temperature increase promotes the formation of plastic kink bands at high temperature.

Table 3
Mechanical properties of the equivalent orthotropic material – Quasi-isotropic CG/PEEK laminates.

	E_x (GPa)	E_y (GPa)	G_{xy} (GPa)	ν_{xy}	C_I (GPa^{-1})
RT	49.58	49.58	15.76	0.289	0.0215
150 °C	45.55	45.55	14.48	0.266	0.0236

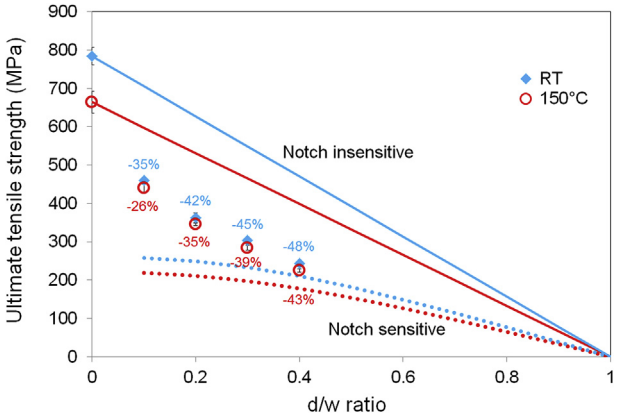

Fig. 6. Influence of temperature on the residual strength of Open-Hole-Tensile laminates.

3.2. Tensile and compressive failure behavior in open hole specimens

Before estimating the influence of matrix ductility on fracture toughness in tension and in compression, it seems relevant to in vestigate the effect of a temperature increase on the failure mechanisms in Open Hole specimens. In unnotched quasi isotropic laminates sub jected to tensile loadings, the mechanical load is primarily (about 73%) borne by the 0° fibers bundles [4] hence justifying a low temperature dependence of the mechanical response. In compression, the specific damage mechanisms associated with compressive loading (local mi crobuckling, formation of a plastic kink band) results from the locally ductile behavior of the PEEK matrix which is enhanced by a tempera ture increase. In open hole specimens, temperature does not influence the hole sensitivity in tension and compression though the failure me chanisms are different. In OHT specimens, the mode I translaminar failure is the primary failure mode. It results from the breakage of fibers bundles in 0° and 45° oriented plies as well as the pull out of 45° fibers bundles in the 45° oriented plies (see Fig. 8). X Rays tomographic ob servations show that the 0° and 45° oriented plies have different con tribution to the fracture behavior of quasi isotropic CG/PEEK laminates (see Fig. 9). A translaminar crack can be observed in 0° plies (see Fig. 9a) suggesting the catastrophic failure of 0° fiber bundles initiated from the stress concentration in the vicinity of the hole (see Fig. 9c). In 45° oriented plies, the fracture surface reveals that splitting

Table 2
Mechanical properties in tension and compression of unnotched CG/PEEK quasi-isotropic laminates depending on testing temperature.

	Tension			*Compression*		
	E_x (GPa)	σ^u_x(MPa)	ε^u_x (%)	E_x (GPa)	σ^u_x (MPa)	ε^u_x (%)
RT	52.57 ± 0.58	784 ± 22	1.52 ± 0.04	49.25 ± 0.50	573 ± 13	1.75 ± 0.07
150 °C	48.30 ± 1.16	664 ± 29	1.33 ± 0.08	47.75 ± 1.20	434 ± 22	1.36 ± 0.04

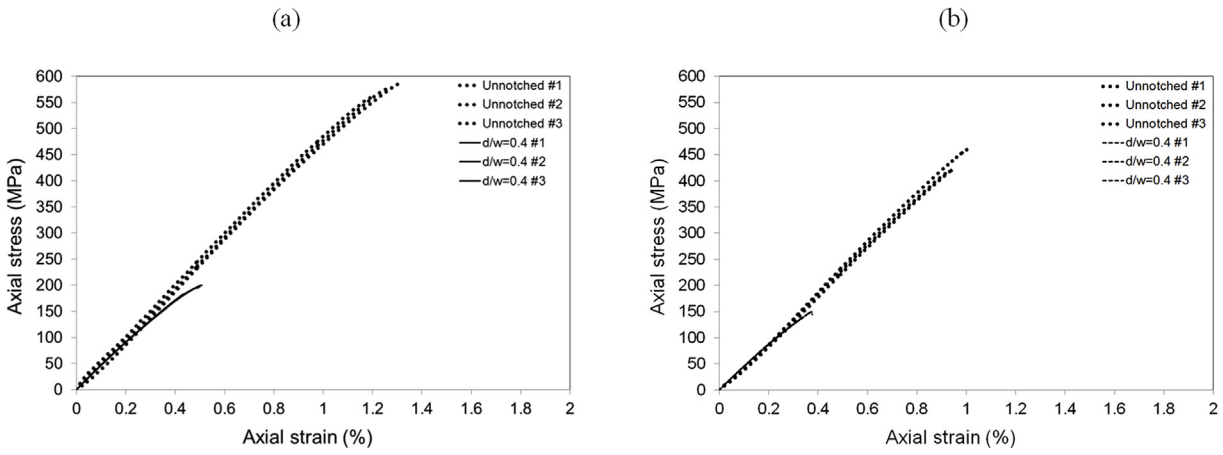

Fig. 7. Mechanical response of Open-Hole specimens with different ratio d/w subjected to compression: (a) RT – (b) 150 °C.

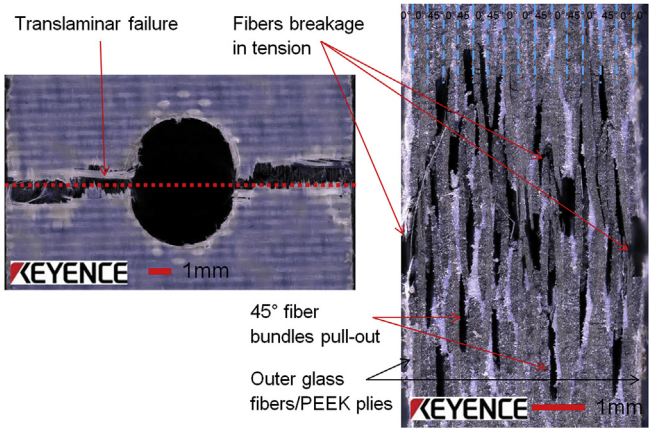

Fig. 8. Microscopic observations of Open-Hole specimens ($d/w = 0.3$) subjected to tension.

(longitudinal intralaminar matrix cracking) occurs in the 45° fibers bundles located in the overstressed region near the hole (see Fig. 9b). Further from the hole edge, 45° broken fibers can be observed as well as 45° fibers pull out along the edges. The onset of translaminar failure occurs when the stress intensity factor in tension reaches its critical value $K_{Ic}^{tension}$ for which both 0° and 45° oriented plies seem to have a specific contribution to the macroscopic translaminar crack (see Fig. 8). Indeed, fracture surface is characterized by the breakage of 0° fiber bundles in 0° plies, whereas it is associated with the breakage of 45° fibers in 45° plies, suggesting that the translaminar cracks follow dif ferent paths depending on fibers bundles orientation.

In OHC specimens, the microscopic observations of the specimen's edges show that the fracture mechanisms are very different depending on the testing temperature. At RT, the breakage of 0° fibers and dela mination are the primary failure modes (see Fig. 10a). They ultimately come along with the crushing of 0° fibers on the outer surfaces of the laminates. A zoom on the damage area reveals that there is no sig nificant micro buckling, but also confirms that failure is driven by the breakage of 0° fibers bundles (see Fig. 11a). At 150 °C, the formation of macroscopic plastic kink band is the primary failure mode (see Figs. 10b and 11b). As indicated in section 3.1, the softening and the ductile behavior of the PEEK matrix is exacerbated at T > Tg. Such behaviors facilitate the initiation of micro buckling at the ply level, resulting in the formation of plastic kink bands. As pointed out in section 1.4, the kink band growth depends on two competing me chanisms. Hole sensitivity being temperature independent in OHC specimens, it suggests that the kink band growth is primarily driven by the critical stress intensity factor in compression $K_{Ic}^{comp.}$. From the pre sent analysis, it is therefore utmost important to evaluate $K_{Ic}^{tension}$ and $K_{Ic}^{comp.}$ at both test temperatures to quantify the energy dissipated during fracture.

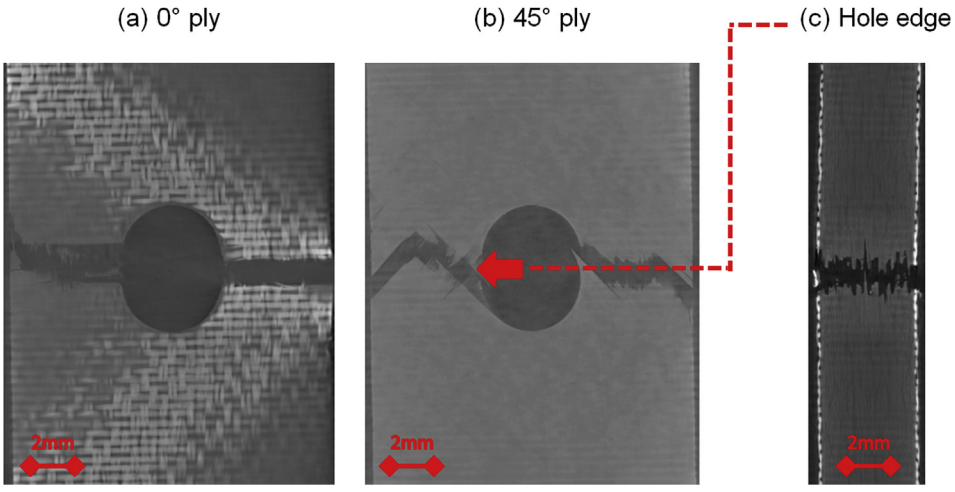

Fig. 9. Tomographic observations of Open-Hole specimens ($d/w = 0.3$) subjected to tension.

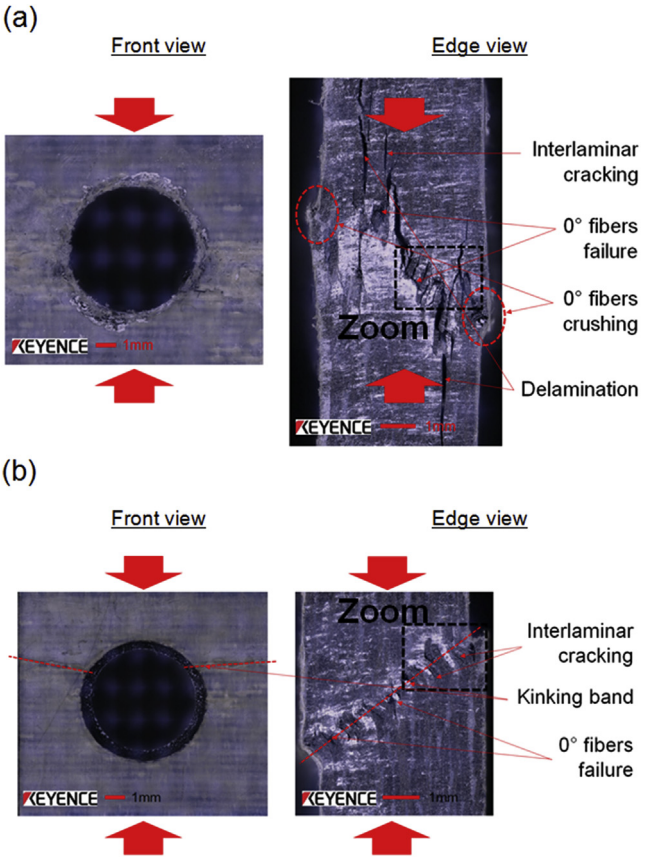

Fig. 10. Front and edge views microscopic observations of Open-Hole-Compression specimens: (a) RT – (b) 150 °C.

3.3. Estimation of the critical fracture toughness in tension $K_{Ic}^{tension}$ and in compression K_{Ic}^{comp}.

The Crack Growth Damage model introduced in section 1.4 can be applied either to Open Hole Tensile (OHT) or to Open Hole Compressive (OHC) specimens [3 5] in order to compute the fracture toughness associated with the translaminar failure of 0° fibers in tension (fibers breakage) $K_{Ic}^{tension}$ and in compression (kink band formation) $K_{Ic}^{comp.}$. The main difficulty primarily consists of determining the length of the critical damage zone c near the hole depending on the stress concentration (hence the hole diameter) in both cases.

In OHT specimens, the damage zone length c obtained from the Average Stress Criterion (see section 1.4) linearly increases as the ratio d/w increases (see Fig. 12). The standard deviation is relatively low at both temperatures. Compared with the values computed at RT, the

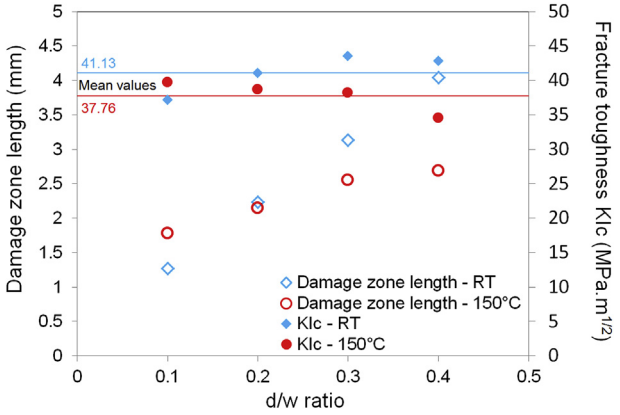

Fig. 12. Influence of temperature on the damage zone length and the fracture toughness in tension $K_{Ic}^{tension}$ from OHT specimens with different ratio d/w

Table 4
Estimation of the mode I fracture toughness in tension from Open-Hole CG/PEEK laminates at RT.

d/w	σ_x^u (MPa)	Damage zone length c (mm)	$F_1(c)$	$F_2(c)$	$K_{Ic}^{tension}$ ($MPa.\sqrt{m}$)	Mean value $K_{Ic}^{tension}$ ($MPa.\sqrt{m}$)
0	784 ± 22	0				
0.1	460 ± 8	1.27	1.26	1.01	37.16	41.13 ± 2.84
0.2	362 ± 13	2.23	1.30	1.04	41.07	
0.3	304 ± 3	3.13	1.32	1.09	43.49	
0.4	244 ± 4	4.04	1.33	1.17	42.79	

Table 5
Estimation of the mode I fracture toughness in tension from Open-Hole CG/PEEK laminates at 150 °C.

d/w	σ_x^u (MPa)	Damage zone length c (mm)	$F_1(c)$	$F_2(c)$	$K_{Ic}^{tension}$ ($MPa.\sqrt{m}$)	Mean value $K_{Ic}^{tension}$ ($MPa.\sqrt{m}$)
0	664 ± 29	0				
0.1	440 ± 10	1.78	1.19	1.02	39.72	37.76 ± 2.28
0.2	345 ± 3	2.14	1.31	1.04	38.66	
0.3	284 ± 6	2.55	1.40	1.07	38.15	
0.4	225 ± 4	2.69	1.50	1.11	34.49	

fracture toughness in tension is about 10% lower at 150 °C (see Table 4 and Table 5), which is consistent with the influence of temperature on the ultimate tensile strength discussed in section 3.2.

In OHC specimens, the idea proposed by Budiansky [28,29] was to calculate the width of the kink band w (in mm) from the properties of

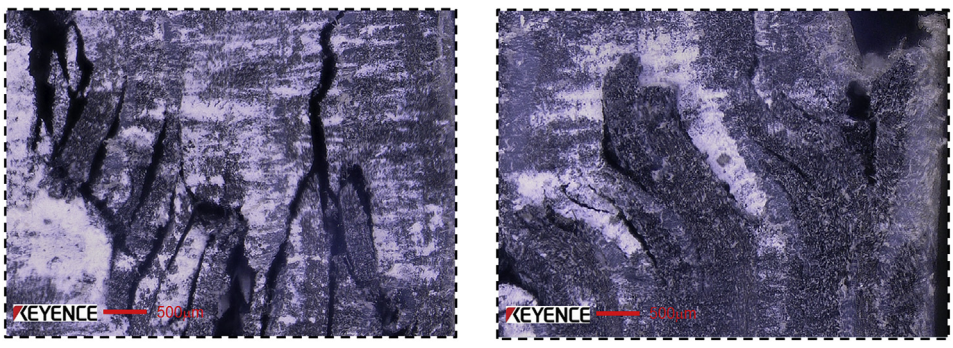

Fig. 11. Zoom on the damage regions of Open-Hole-Compression specimens: (a) RT – (b) 150 °C.

Table 6
Features and properties of carbon-fibers reinforced PEEK laminates.

	Fiber diameter d_f (μm)	Fibers volume fraction V_f	Fiber's Young modulus E_f(GPa)	Compressive strength σ_x^u(MPa)	Compressive modulus E_x(GPa)
RT	7	0.5	230	716	59.4
150 °C	7	0.5	230	542	57.6

Table 7
Estimation of the kink-band width from the Budiansky micromechanics approach applied to orthotropic C/PEEK laminates subjected to compressive loading at RT and 150 °C.

	τ_y(MPa)	Kink-band width w (μm)	$K_{Ic}^{comp.}$ (MPa.$\sqrt{m}$)
RT	112	44	30.59
150 °C	58	55	29.24

Table 8
Estimation of the mode I fracture toughness in compression from Open-Hole CG/PEEK laminates at RT and 150 °C.

		d/w	σ_x^u(MPa)	Kink-band length c (mm)	$K_{Ic}^{comp.}$ (MPa.$\sqrt{m}$)
RT	Crack Growth	0	573 ± 13	0	
	Damage model	0.4	197 ± 3	2.65	35.08
	Budiansky				30.59
150 °C	Crack Growth	0	434 ± 22	0	
	Damage model	0.4	153 ± 7	2.89	27.25
	Budiansky				29.24

both the constitutive elements and the unidirectional fiber reinforced matrix composite (see Fig. 4b):

$$w = 2v_c = \frac{\pi d_f}{4}\left(\frac{V_f E_f}{2\tau_y}\right)^{1/3} \tag{16}$$

d_f is the fiber diameter, V_f is the fiber volume fraction, E_f is the fiber elastic modulus and τ_y is the in plane shear yield stress of the unidirectional fiber reinforced matrix composite (see Table 6). From the computation of the mode I critical strain energy release $G_{Ic}^{comp.}$ by Eq. (13), it is therefore possible to determine the kink band toughness $K_{Ic}^{comp.}$ (see Table 7) for an orthotropic plate under plane stress conditions according to Eq. (5). The values obtained from the Budiansky approach are similar to the ones computed from the CDG model introduced in section 1.4 (see Table 8). However the agreement between the values seems to be better at 150 °C as the formation of kink band is the primary failure mode contrary to what is observed at RT as discussed in section 3.2. This failure mechanism could also explain the decrease (about 20%) of $K_{Ic}^{comp.}$ as temperature increases.

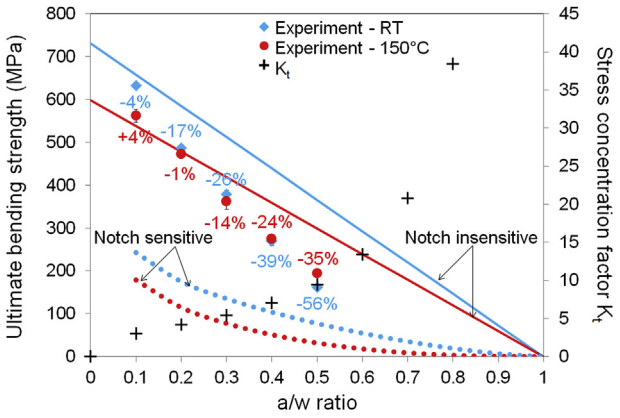

Fig. 13. Evolution of the residual strength and the stress concentration factor in SENB specimens: influence of temperature and initial ratio.a/w

3.4. Fracture behavior of SENB specimens

The influence of temperature on the residual strength is limited except for a ratio $a/w = 0.5$ for which a temperature increase contributes to a 20% increase of the bending strength (see Table 9). The influence of stress concentration on the residual strength (indicated in % on Fig. 13) is lower at high temperatures with a maximum decrease of 35 56% with respect to the notch insensitive case. Contrary to what was observed in OHT specimens, it also suggests that notch sensitivity is temperature dependent in SENB specimens, probably due to the contribution of compressive failure (the formation ok kink band is temperature dependent) to the failure in bending [32].

Based on a Digital Image Correlation analysis, the longitudinal strain distribution at the surface of SENB specimens can be computed from the Vic2D software. It appears that the upper part of specimens is subjected to compression whereas the lower part is subjected to tension (see Fig. 14). In addition, a tomographic observation of the 0° plies reveals a local crushing of laminates' upper edges in the contact area with upper cylinder. As a/w ratio increases (typically from $a/w = 0.3$), the stress concentration factor K_t increases as well (see Fig. 13), and promotes a translaminar failure dominated by the tensile breakage of 0° carbon fibers. No visible damage can be observed on upper edges of these specimens as the bending stress is lower than the crushing stress [32]. As introduced in section 1.2, $a_{tension}$ and $a_{comp.}$ are the equivalent crack lengths associated with tension and compression respectively (see Fig. 14), illustrating that SENB specimens experience both tensile and

Table 9
Prediction of the ultimate strength of quasi-isotropic CG/PEEK laminates subjected to three points bending at RT – Computation from the mode I critical fracture toughness in tension at RT and 150 °C.

	$F(a/w)$	RT		150°C		Influence of T° on σ_x^u exp.
		σ_x^uexp. (MPa)	σ_{remote}^u predicted (MPa)	σ_x^uexp. (MPa)	σ_{remote}^u predicted (MPa)	
0		731 ± 5		598 ± 14		
0.1	1.01	632 ± 6	595 (6%)	562 ± 6	546 (3%)	12%
0.2	1.03	486 ± 10	429 (13%)	472 ± 19	394 (19%)	2%
0.3	1.05	377 ± 10	331 (14%)	361 ± 5	304 (19%)	4%
0.4	1.18	269 ± 6	254 (6%)	274 ± 2	233 (17%)	+2%
0.5	1.42	162 ± 8	189 (+14%)	193 ± 4	174 (11%)	+19%

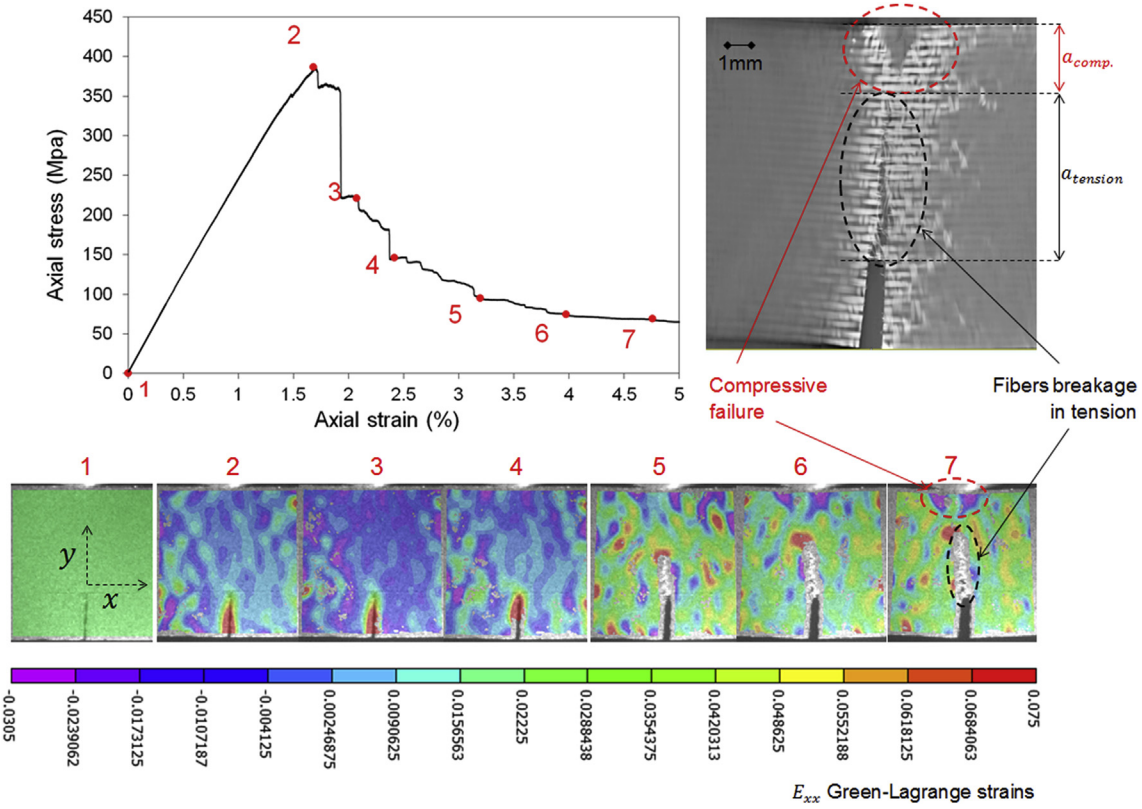

Fig. 14. Evolution of the longitudinal Green-Lagrange strain distribution and the translaminar crack in SENB specimens at 150 °C ($a/w = 0.3$): (a) macroscopic mechanical response – (b) tomographic observation of the 0° fibers plies

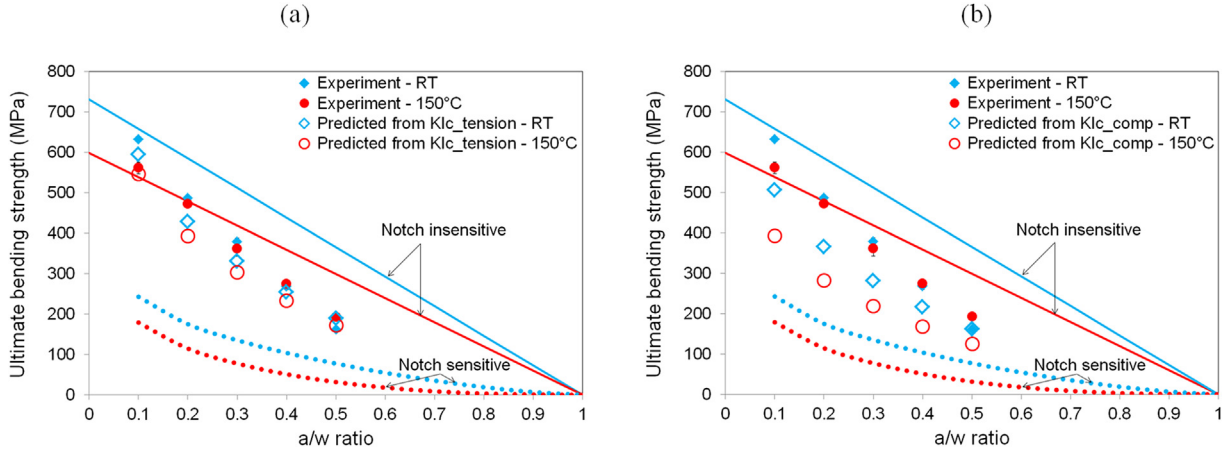

Fig. 15. Comparison of the predicted and experimental residual strengths of SENB specimens with different ratio a/w: (a) from $K_{Ic}^{tension}$ – (b) from.$K_{Ic}^{comp.}$

compressive failure. Finally, based on the estimation $K_{Ic}^{tension}$ and $K_{Ic}^{comp.}$ computed in section 3.3, the ultimate strength of SENB specimens σ_{remote}^{u} can be predicted from Eq. (4) with a relatively good accuracy in com parison with the results obtained from the critical fracture toughness in compression (see Table 9 and Fig. 15).

4. Conclusions

In the framework of the Linear Elastic Fracture Mechanics, the main purpose of this work was to predict the ultimate strength of Single Edge Notch Bending quasi isotropic laminates consisting of hybrid carbon/glass/PEEK thermoplastic composites intended to be used in aeronautics in high temperature service conditions ($T > T_g$). The main conclusions are summarized as follows:

- Translaminar failure is the primary failure mode in SENB specimens which experience simultaneous tensile and compressive quasi brittle failures. At both test temperatures, failure is driven by the breakage of 0° and 45° oriented fibers in tension as well as the formation of kink bands in compression.
- Compressive failure being primarily matrix dominated (hence tem perature dependent), failure in bending (hence the corresponding fracture toughness) is modified by a temperature increase.
- A simple model derived from fracture mechanics concepts combined with a critical damage zone (determined from the Average Stress Criterion) has been implemented. It was applied to quantify the critical fracture toughness in tension $K_{Ic}^{tension}$ and in compression $K_{Ic}^{comp.}$ based on experimental data obtained from Open Hole Tensile and Compressive tests conducted at room temperature and 150 °C

($T > T_g$).

- The ultimate strength of TP thermoplastic composites structures is simply predicted with a relatively good accuracy from the critical fracture toughness in tension and compression.

The present study is expected to be a contribution towards the design of high performance TP laminates for aeronautical applications under high temperature conditions.

References

[1] Awerbuch J, Madhukar MS. Notched strength of composite laminates: predictions and experiments – a review. J Reinforc Plast Compos 1985;4:3–159.
[2] Soutis C, Curtis PT. A method for predicting the fracture toughness of CFRP laminates failing by fibre microbuckling. Composites Part A 2000;31:733–40.
[3] Borkowski L, Kumar RS. Inverse method for estimation of composite kink-band toughness from open hole compression strength data. Compos Struct 2018;186:183–92.
[4] Vieille B, Chabchoub M, Bouscarrat D, Keller C. Prediction of the notched strength of woven-ply PolyPhenylene Sulfide thermoplastic composites at a constant high temperature by a physically-based model. Compos Struct 2016;153:529–37.
[5] Belmonte HMS, Ogin SL, Smith PA, Lewin R. A physically-based model for the notched strength of woven quasi-isotropic CFRP laminates. Composites Part A 2004;35(7–8):763–78.
[6] Tan SC. Stress concentration in laminated composites. Lancaster, Pa: Technomic Pub. Co.; 1994.
[7] Reinoso J, Arteiro A, Paggi M, Camanho PP. Strength prediction of notched thin ply laminates using finite fracture mechanics and the phase field approach. Compos Sci Technol 2017;150:205–16.
[8] Su ZC, Tay TE, Ridha M, Chen BY. Progressive damage modeling of open-hole composite laminates under compression. Compos Struct 2015;122:507–17.
[9] Xiao J, Bathias C. Damage and fracture of notched non-woven and woven composite laminates. Compos Sci Technol 1994;52:99–108.
[10] Whitney JM, Nuismer RJ. Stress fracture criteria for laminated composites containing stress concentrations. J Compos Mater 1974;8:253–65.
[11] Nuismer RJ, Whitney JM. Uniaxial failure of composite laminates containing stress concentration. ASTM STP 1975;593:117–42.
[12] Naik NK, Shembekar PS. Notched strength of fabric laminates I: prediction. Compos Sci Technol 1992;44:1–12.
[13] Kim JK, Kim DS, Takeda N. Notched strength and fracture criterion in fabric composite plates containing a circular hole. J Compos Mater 1995;29:982–98.
[14] Waddoups ME, Eisenmann JR, Kaminski BE. Macroscopic fracture mechanics of advance composite material. J Compos Mater 1971;5:446–54.
[15] Bowie OL. Analysis of an infinite plate containing radial cracks originating at the boundary of an internal circular hole. J Math Phys 1956;25(1):60–71.
[16] Afaghi-Khatibi A, Ye L, Mai YW. An effective crack growth model for residual strength evaluation of composite laminates with circular holes. J Compos Mater 1996;30:142–63.
[17] Wu EM. Fracture mechanics of anisotropic plates. Composite materials workshop. Technomic Publishing Co.; 1968.
[18] Camanho PP, Maimí P, Dávila CG. Prediction of size effects in notched laminates using continuum damage mechanics. Compos Sci Technol 2007;67(13):2715–27.
[19] Tada H, Paris PC, Irwin GR. The stress analysis of cracks handbook. third ed. January: ASME Press; 2000.
[20] Tan SC. Stress concentration in laminated composites. Lancaster, Pa: Technomic Pub. Co.; 1994.
[21] Lisle T, Bouvet C, Hongkarnjanakul N, Pastor M-L, Rivallant S, Margueres P. Measure of fracture toughness of compressive fiber failure in composite structures using infrared thermography. Compos Sci Technol 2015;112:22–33.
[22] Laffan MJ, Pinho ST, Robinson P, McMillan AJ. Translaminar fracture toughness testing of composites: a review. Polym Test 2012;31(3):481–9.
[23] Soutis C, Fleck NA, Smith PA. Failure prediction technique for compression loaded carbon fibre–epoxy laminate with an open hole. J Compos Mater 1991;25:1476–98.
[24] Soutis C, Fleck NA. Static compression failure of carbon fibre T800/924C composite plate with a single hole. J Compos Mater 1990;24:536–58.
[25] Soutis C, Curtis PT, Fleck NA. Compressive failure of notched carbon fibre composites. Proc Roy Soc Lond A 1993;440:241–56.
[26] Soutis C. Damage tolerance of open-hole CFRP laminates loaded in compression. Compos Eng 1994;4(3):317–27.
[27] Sih GC, Chen EP. Cracks in composite materials. Sih GC, editor. Mechanics of fracture, vol. 6. London: Martinus Nijoff Publishers; 1981.
[28] Budiansky B, Fleck NA. Compressive kinking of fiber composites: a topical review. Appl Mech Rev 1994;47(6):S246–70.
[29] Jelf PM, Fleck NA. Compression failure mechanisms in unidirectional composites. J Compos Mater 1992;26(18):2706–26.
[30] Rice JR. Liebowitz H, editor. Mathematical analysis in the mechanics of fracture, vol. 2. New York: Academic Press; 1968. Chap. 3.
[31] Dubary N, Taconet G, Bouvet C, Vieille B. Influence of temperature on the impact behavior and damage tolerance of hybrid woven-ply thermoplastic laminates for aeronautical applications. Compos Struct 2017;168:663–74.
[32] Vieille B, Gonzalez J-D, Bouvet C. Fracture mechanics of hybrid composites with ductile matrix and brittle fibers: influence of temperature and constraint effect. J Compos Mater 2018. https://doi.org/10.1177/0021998318802613.
[33] Krishnaraj V, Zitoune R, Davim JP. Drilling of polymer-matrix composites. In: Davim JP, editor. Springer briefs in applied sciences and technology, Manufacturing and surface engineering. Springer-Verlag Berlin and Heidelberg GmbH & Co. KG Publisher; 2013.
[34] Vieille B, Albouy W, Taleb L. Investigations on stamping of C/PEEK laminates: influence on meso-structure and macroscopic mechanical properties under severe environmental conditions. Composites Part B 2014;63:101–10.
[35] Test standard EN 6035, aerospace series - fiber-reinforced plastics - test method - determination of notched and unnotched tensile strengthPublished by the European association of aerospace industries (AECMA). April 1996.
[36] Vieille B, Chabchoub M, Bouscarrat D, Gautrelet C. A fracture mechanics approach using Acoustic Emission technique to investigate damage evolution in woven-ply thermoplastic structures at temperatures higher than glass transition temperature. Composites Part B 2017;116:340–51.